

# Effective sugar-derived organic gelator for three different types of lubricant oils to improve tribological performance

Ruochong ZHANG<sup>1,2</sup>, Xuqing LIU<sup>3</sup>, Zhiguang GUO<sup>1,4</sup>, Meirong CAI<sup>1,\*</sup>, Lei SHI<sup>1,\*</sup>

<sup>1</sup> State Key Laboratory of Solid Lubrication, Lanzhou Institute of Chemical Physics, Chinese Academy of Sciences, Lanzhou 730000, China

<sup>2</sup> University of Chinese Academy of Sciences, Beijing 100049, China

<sup>3</sup> School of Materials, University of Manchester, Oxford Road, Manchester M13 9PL, UK

<sup>4</sup> Hubei Collaborative Innovation Centre for Advanced Organic Chemical Materials and Key Laboratory for the Green Preparation and Application of Functional Materials (Ministry of Education), Hubei University, Wuhan 430062, China

Received: 19 July 2017 / Revised: 30 September 2018 / Accepted: 06 July 2019

© The author(s) 2019.

**Abstract:** In this study, the gelling ability and lubrication performance of N-octadecyl-D-gluconamides (NOG) in liquid paraffin (LP), pentaerythritol oleate (PE-OA), and polyethylene glycol (PEG) oils were systemically investigated. The NOG, which could gelate the investigated oils, was successfully synthesized by a one-step method. The prepared gel lubricants were completely thermoreversible and exhibited improved thermal stability, according to the thermogravimetry analysis (TGA) reports. Rheological tests confirmed that the NOG gelator could effectively regulate the rheological behavior of the base oils. Tribological evaluation suggested that NOG, as an additive in the three types of base oils, could remarkably reduce the friction and wear in steel contacts. A plausible mechanism for the improved performances was proposed based on the mechanical strength of the gels and the formation of the boundary-lubricating film on the worn surface. The results indicated that NOG is a potential gelator for preparing gel lubricants with excellent tribological properties and environment-friendly characteristics.

**Keywords:** gel lubricant; supermolecular assembly; rheological property; tribological performance; lubricating mechanism

## 1 Introduction

Friction and wear occur in different forms in industry, causing tremendous energy loss and premature failure of key mechanical components, thus dramatically lowering the production efficiency. Therefore, research and development of novel lubricants has drawn sustained attention from researchers and engineers [1]. Compared with solid lubricants, advantages such as long lubricating life, low work noise, and good heat dissipation performance promote the wide application of fluid lubricants [2, 3]. Lubricating oils and lubricating greases are two basic fluid lubricants that are commonly used in industry. Oils with good fluidity are able to

maintain a continuous lubricating film within the narrow contact interface but are prone to leakage and loss [4]. Therefore, various greases, with improved anti-fouling, sealing, and anti-oxidation abilities, have been developed to circumvent the leakage issue of oils [5]. However, the viscosity characteristics still limit the use of greases in the confined space [6].

For finding novel lubricating materials that can combine the merits of oils and greases, additives that can regulate the rheological behavior of lubricants have been utilized [7–10]. The low molecular weight organic gelator (LMWG) is a type of widely used agent that confers excellent thixotropic properties to lubricating oils. The first thermo-reversible lubricating gel, as

\* Corresponding authors: Meirong CAI, E-mail: caimr@licp.cas.cn; Lei SHI, E-mail: leishi@licp.cas.cn

reported by Takahashi et al. [11] was prepared using an amide compound as gelling agent in the base fluid. Compared with the base oil, the lowered coefficient of friction (COF) of lubricating gel was attributed to the adsorption of LMWGs on the metal surface. Cai et al. [7] successfully synthesized functional ionogelators with anticorrosive and antioxidative performance, effectively solving the issue of corrosion in ionic-liquids (ILs)-based lubricants. The amino-acid-based LMWGs were shown to effectively promote the tribological performance of mineral oils, synthetic oils, and water [12, 13]. Huang et al. [14] found that the poly-hydroxyl LMWG exhibits a remarkable antiwear performance for a wide range of frictional pairs, including steel/steel, steel/aluminum, steel/copper, and steel/ $\text{Al}_2\text{O}_3$ , and this universal antiwear ability was ascribed to the robust physical absorption film formed by the gelator. Although gel lubricants have been widely investigated in the past few years, the relationships between the lubrication performance and corresponding rheological properties have been rarely examined. Furthermore, in recent years, environmental concerns and increasingly strict regulations are driving the use of environment-friendly lubricants, thereby increasing the demand for compatible gelators as well.

In this paper, novel gel lubricants with N-octadecyl-D-gluconamide (NOG) gelator were prepared via a facile method, which is in accordance with the concept of green chemistry for non-toxic reactants and environment-friendly synthetic processes. The self-assembly behavior, thermal performance, and rheological properties of the gel lubricants with a given content of NOG were investigated. In addition, the lubrication performance and tribological mechanism of gel lubricants based on liquid paraffin (LP) (as a representative hydrocarbon oil), pentaerythritol oleate (PE-OA) (as a representative ester oil), and polyethylene glycol (PEG) (as a representative ether alcohol oil) were studied.

## 2 Experimental

### 2.1 Materials

N-octadecylamine and  $\delta$ -glucolactone, which serve as the reactants for the NOG synthesis, were purchased from Energy Chemical. Methanol was purchased from Cinc High Purity Solvents (Shanghai) Co. Ltd. Liquid paraffin was purchased from Tianjin Bai Shi Chemical Co. Ltd. PEG400 was purchased from Tianjin Kemiou Chemical Reagent Co. Ltd. and pentaerythritol oleate was synthesized following a previous study [15]. All the other chemicals used in the present study were of AR grade. Deionized water was used through the entire experiment.

### 2.2 Preparation of NOG

NOG was synthesized according to a previously reported protocol [16]. Briefly, 20 mmol  $\delta$ -glucolactone was dissolved in 100 mL methanol at 60 °C, and then added to a mixture of methanol (50 mL) and n-octadecylamine (20 mmol). The mixture was maintained stirred for 3 h to allow for the completion of reaction. The white precipitation thus produced was filtered out, recrystallized thrice with methanol, and finally dried in a vacuum-drying oven. The scheme of NOG gelator synthesis is illustrated in Fig. 1.

### 2.3 Preparation of gel lubricants

The gel lubricants were prepared using the following steps. The NOG gelator was added to different types of base oils at a given mass concentration. After heating and stirring, the NOG gelator was completely dissolved in base oils, producing a transparent solution. The gel was then formed by leaving the homogeneous liquids undisturbed during the cooling process. The gels formulated with the investigated base oils and the NOG gelator are respectively denoted as PE-OA-NOG, PEG400-NOG, and LP-NOG.

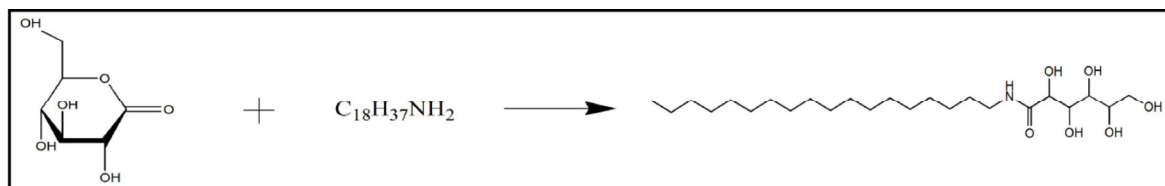


**Fig. 1** Schematic illustration of the preparation processes of NOG gelator.

## 2.4 Characteristics

The structure of NOG was investigated via proton nuclear magnetic resonance ( $^1\text{H}$  NMR INOVA-400 Hz) and carbon nuclear magnetic resonance ( $^{13}\text{C}$  NMR INOVA-100 MHz). Nicolet iS10 FTIR spectrometer was used to study the interactions of the NOG molecules in the LP base oil. The thermal stability of NOG and the gel lubricants was investigated by STA 449C Jupiter simultaneous TG-DSC, from 25 °C to approximately 800 °C, with a heating rate of 10 °C per min in air. The rheological properties of the gel lubricants were measured using a RS6000 Rheometer (0.01–1,000 Pa, 1 Hz, 20 °C).

## 2.5 Tribological tests

Tribological performance of the gel lubricants was evaluated on steel/steel friction pairs using optimal SRV-IV oscillating reciprocating friction and wear tester. The wear volumes of worn scars on the steel discs were investigated using Microxam 3D non-contact surface profiler. JSM-5600LV SEM and PHI-5702 multifunctional XPS were used to characterize the morphology and chemical composition of worn scars lubricated by corresponding lubricants.

## 3 Results and discussion

### 3.1 Structure of NOG

The results of the NOG structure investigated by  $^1\text{H}$  NMR and  $^{13}\text{C}$  NMR are shown as follows:

$^1\text{H}$  NMR (400 MHz,  $\text{DMSO-d}_6$ )  $\delta/\text{ppm}$ : 7.59 (t,  $J = 5.7$  Hz, 1H), 5.34 (d,  $J = 5.1$  Hz, 1H), 4.53 (d,  $J = 4.6$  Hz, 1H), 4.46 (d,  $J = 4.9$  Hz, 1H), 4.38 (d,  $J = 7.2$  Hz, 1H), 4.32 (t,  $J = 5.7$  Hz, 1H), 4.05–3.34 (m, 6H), 3.16–2.91 (m, 2H), 1.39 (s, 2H), 1.23 (s, 30H), 0.85 (t,  $J = 6.7$  Hz, 3H).

$^{13}\text{C}$  NMR (101 MHz,  $\text{DMSO-d}_6$ )  $\delta/\text{ppm}$ : 172.18, 73.60, 72.39, 71.47, 70.10, 63.36, 38.22, 31.26, 29.14, 29.01, 28.79, 28.66, 26.35, 22.06, 13.92.

### 3.2 Gelation process of the gel lubricants

Images of the gelation process of PEG400 (Fig. 2(a)), LP (Fig. 2(b)), and PE-OA (Fig. 2(c)) with 3% NOG were recorded using a digital camera. Figure 2 shows that the white floccule first appears at the bottom of

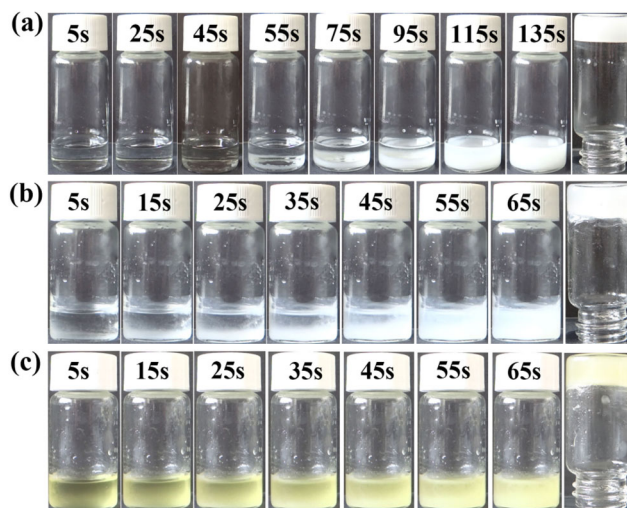


**Fig. 2** Formation process of gel lubricants based on (a) PEG400, (b) LP, and (c) PE-OA, with 3% NOG.

the sample bottle, corresponding to the occurrence of gelation in this region that has relatively lower temperature. With the NOG continuously separating out from the base oil during the cooling process, the system eventually transforms into a semi-solid gel state. All the study oils could be transformed into the gel state within 3 min, indicating the high gel-forming ability of NOG gelator.

### 3.3 Gel formation mechanism

According to previous studies, IR is a simple and effective method to show the existence of hydrogen bonds [17, 18]. The IR spectra of LP with varied NOG content were investigated to probe the interaction of the NOG molecules in blank oil. According to a previous report, the hydroxyl groups exist in a free state in dilute inert solvent, and the corresponding stretching band belongs to 3,640–3,610  $\text{cm}^{-1}$ , with a sharp narrow peak on the spectrum. The spectra of hydroxyl group broaden remarkably and move to a lower wave number with the formation of intramolecular or intermolecular hydrogen bonds [19]. Figure 3 shows that the hydroxyl group peaks shift to lower wave numbers and become broader upon addition of 3% NOG to LP, corresponding to the dimer (3,513  $\text{cm}^{-1}$ ) and multimer (3,327  $\text{cm}^{-1}$ ) of NOG. With a further increase in the NOG concentration, the peaks become wider with a lower wavenumber (3,507  $\text{cm}^{-1}$  and 3,316  $\text{cm}^{-1}$ ), and the dimer peak is gradually covered by that of multimer when the NOG concentration increases to 10%, producing a single

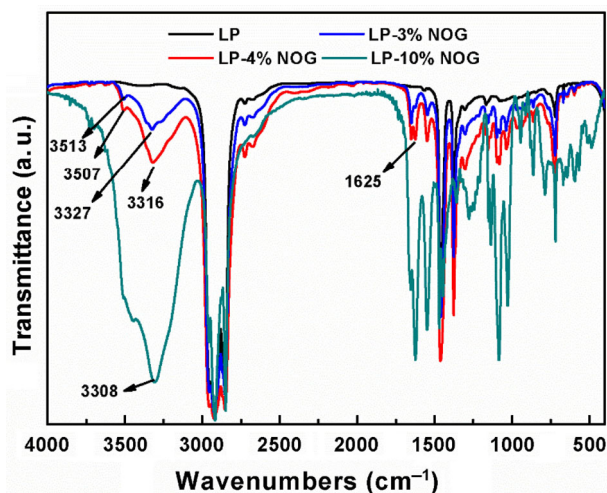


**Fig. 3** FTIR spectra of LP with varied content of NOG gelator.

wide peak at  $3,308\text{ cm}^{-1}$ . Moreover, the stretching band of the carbonyl group in amine acid normally appears at  $1,690\text{ cm}^{-1}$ . As shown in Fig. 3, the corresponding peak appears at  $1,625\text{ cm}^{-1}$ , indicating the formation of hydrogen bonds among the carbonyl groups [20]. The variation in IR spectra indicates that the NOG molecules separate from LP during the cooling process and, at the same time, they assemble into dimers and multimers through hydrogen bond interactions among hydroxyl groups and carbonyl groups.

### 3.4 Thermal performances

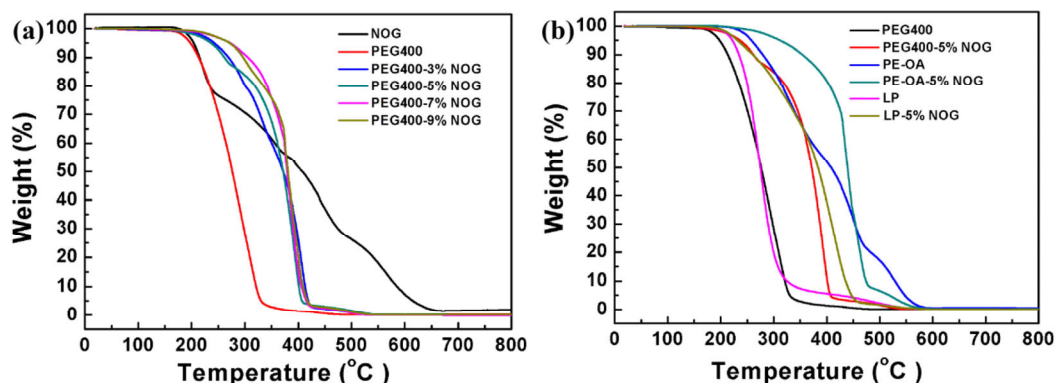
The thermal stability of the prepared gel lubricants was investigated by TGA. As shown in Fig. 4(a), the decomposition temperature of PEG400 was higher than  $200\text{ }^{\circ}\text{C}$  and the corresponding gels with varied NOG content showed a higher decomposition temperature than that of pure PEG400. As shown in

the curve in Fig. 4(b), all three types of gel lubricants exhibit better thermal stability than that of the corresponding base oil. The temperatures for 30% weight loss of gel lubricants are summarized in Table S1 in the Electronic Supplementary Material (ESM), showing that the NOG gelator could effectively improve the thermal stability of base oils.

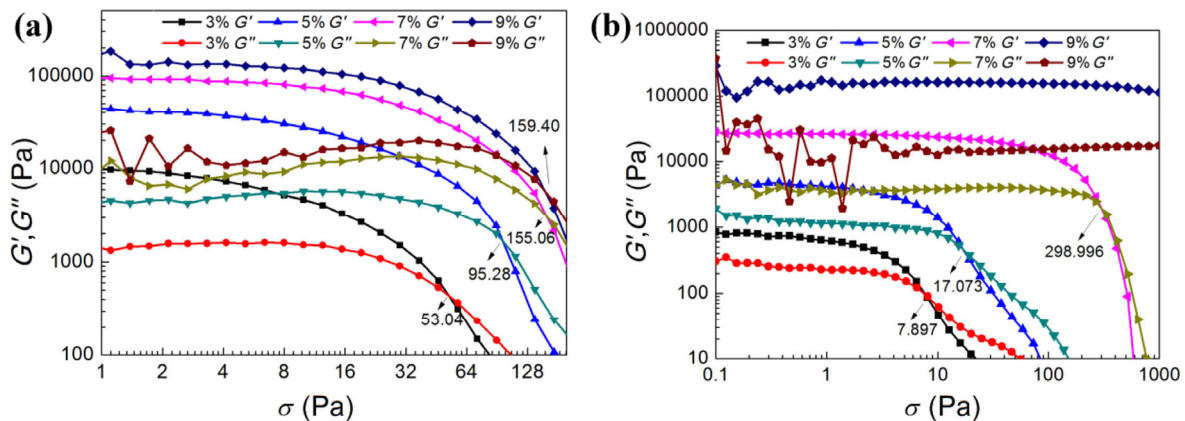
### 3.5 Rheological properties

Figure 5(a) shows that both storage moduli ( $G'$ ) and loss moduli ( $G''$ ) of PEG400 gel were a function of stress.  $G'$  increases from nearly  $10\text{ kPa}$  to more than  $100\text{ kPa}$  upon an increase in NOG concentration from 3% to 9%, with the corresponding critical stress also rising from  $53.04$  to  $159.40\text{ Pa}$ . The LP gels exhibit a similar tendency of variation with PEG400 gel, as presented in Fig. 5(b). Two properties could be concluded from the rheological performance. First, the values of  $G'$  and critical stress for different gel lubricants increase with the content of NOG, indicating that mechanical stability and the flow resistance of LP gel are effectively enhanced with an increase in NOG concentration. Second, all the gel lubricants with varied content of NOG gelator show the shear-thinning property.

Similar to PEG400 and LP gels, the  $G'$  of PE-OA was larger than  $G''$  when the stress was lower than the critical stress, as shown in Fig. 6. The value of  $G'$  increases from  $160$  to nearly  $600\text{ Pa}$ , with the corresponding critical stress increasing from  $0.7439$  to  $2.0457\text{ Pa}$ , with increasing NOG content, which also shows mechanical stability, good tolerance ability, and shear-thinning property. However, the rheological



**Fig. 4** (a) TGA curves of NOG gelator and gel lubricants based on PEG400 with different concentrations of NOG, (b) TGA curves of three different base oils and the corresponding gel lubricants.



**Fig. 5** Rheological property of (a) PEG400 and (b) LP gels investigated by the relationship between  $G'$ ,  $G''$  and the applied shear stress.

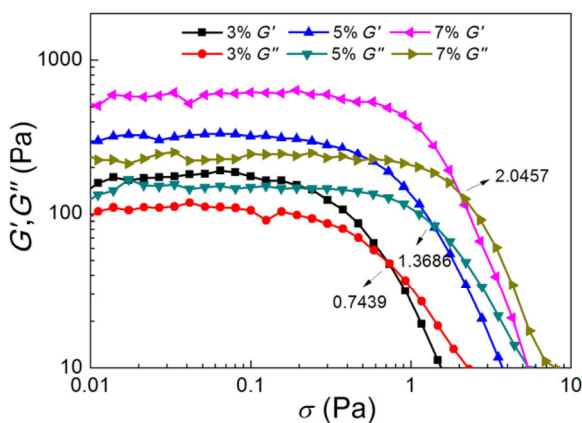


**Fig. 6** Rheological property of PE-OA gels investigated by the relationship between  $G'$ ,  $G''$  and the applied shear stress.

behavior of PE-OA gels showed that the gel structure is prone to destruction by shear stress, and not as stable as that of PEG400 and LP gels, likely because the molecular volume of PE-OA is too big for the NOG gelator to be hold. In summary, the thermal stability and rheological behavior of three lubricating oils were simultaneously enhanced by the addition of NOG gelator.

### 3.6 Tribological performances

A systemic investigation of the effect of NOG concentration in the prepared gel lubricants on the mean COF, mean WV, and friction curves was carried out, as reported in this section [21, 22].

#### 3.6.1 Tribological performance of LP gel lubricants

According to the lubrication performance of LP gel presented in Figs. 7(a) and 7(b), the mean COF and

wear volume gradually decrease to the lowest value when the content of NOG reaches to 2 wt%. To further investigate the lubrication capacity of LP-2% NOG gel under severe conditions, the load ramp test and frequency ramp test were performed as shown in Figs. 7(c) and 7(d). The COFs of LP increased above 0.20 with large fluctuations under both test conditions. In contrast, the friction curves of LP-2% NOG gel stabilized at a much lower level during the whole test process, indicating a good adaptability of LP-2% NOG gel for the varying working conditions.

#### 3.6.2 Tribological performance of PE-OA gel lubricants

Figure 8 presents the results of tribological evaluation of PE-OA gels and PE-OA oil. As shown in Fig. 8(a), the COF reaches the minimum value at the NOG concentration of 4%. Figure 8(b) shows that the COF curves of blank PE-OA and PE-OA-2% NOG present a clear running-in period during the initial stage of the friction test, indicating the relatively poor lubrication ability. When the NOG concentration was more than 3%, the curve of COF was smooth without the abnormally high friction during the running-in periods. The WV and maximum depth of worn scars were used (Figs. 8(c) and 8(d)) to characterize the anti-wear ability of PE-OA-based gel lubricants. Similar to the variation in COF, the WV was gradually reduced by adding the NOG gelator. The cross-section topographies of the worn scars lubricated by PE-OA-based lubricants in Fig. 9 showed that the worn scars lubricated by PE-OA and PE-OA-2% NOG exhibit a markedly deep groove, and that the deep groove in the steel scar disappears completely once the content of NOG reaches to 3%,

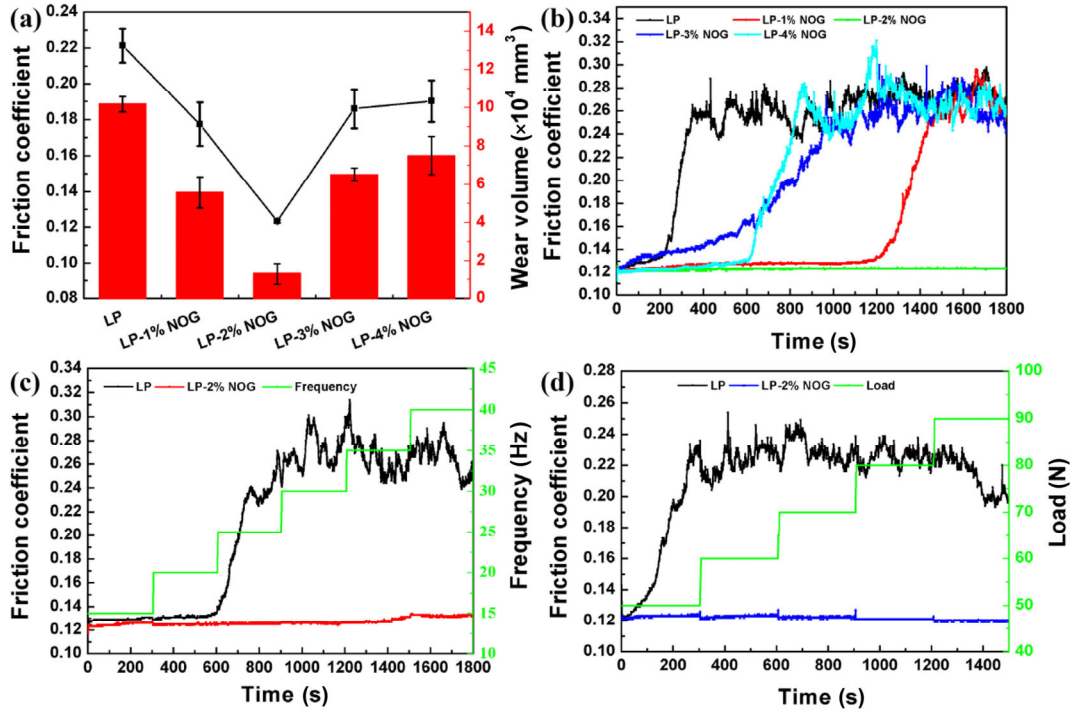


**Fig. 7** (a) Average COF and WV, (b) evolution of COF/time of steel discs lubricated by the LP with different concentrations of NOG at room temperature (SRV: load = 50 N, stroke = 1 mm, frequency = 25 Hz, and duration = 30 min). Evolution of COF/time (c) during a frequency ramp test from 15 to 40 Hz (SRV: load = 50 N, stroke = 1 mm, and duration = 30 min), and (d) during a load ramp test from 50 to 90 N (SRV: stroke = 1 mm, frequency = 25 Hz, and duration = 30 min) for LP and gel with 2% NOG.

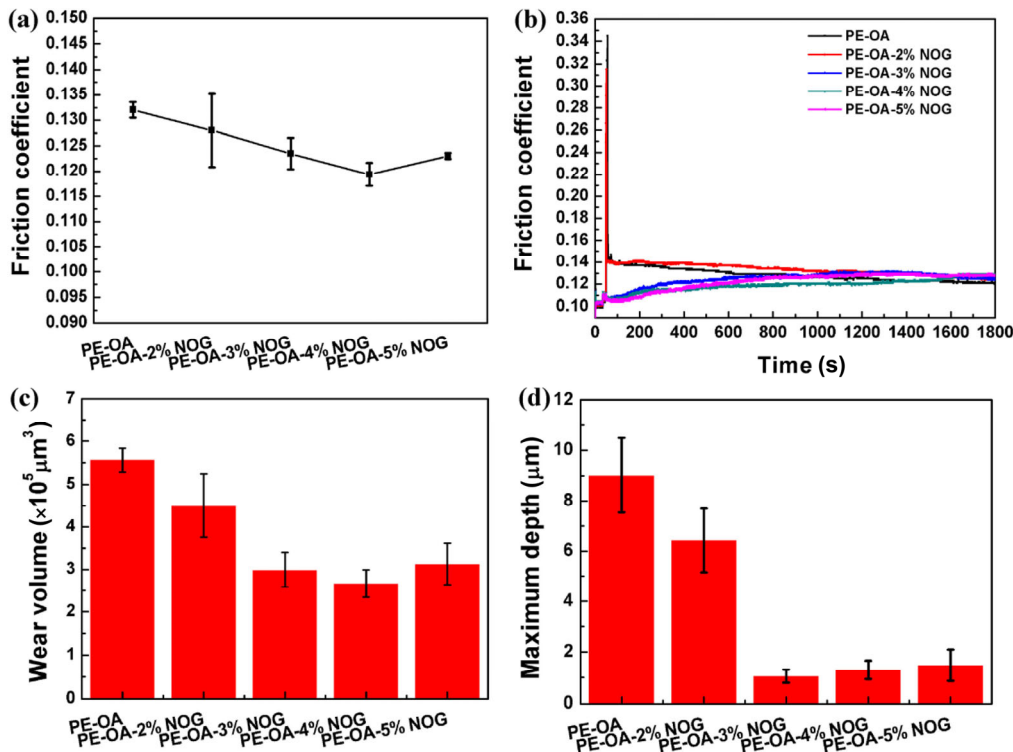


**Fig. 8** (a) Average COFs, (b) friction curves, (c) wear volumes, and (d) maximum depth of worn scars lubricated by the PE-OA and corresponding gel lubricants at room temperature (SRV: load = 300 N, stroke = 1 mm, frequency = 15 Hz, and duration = 30 min).

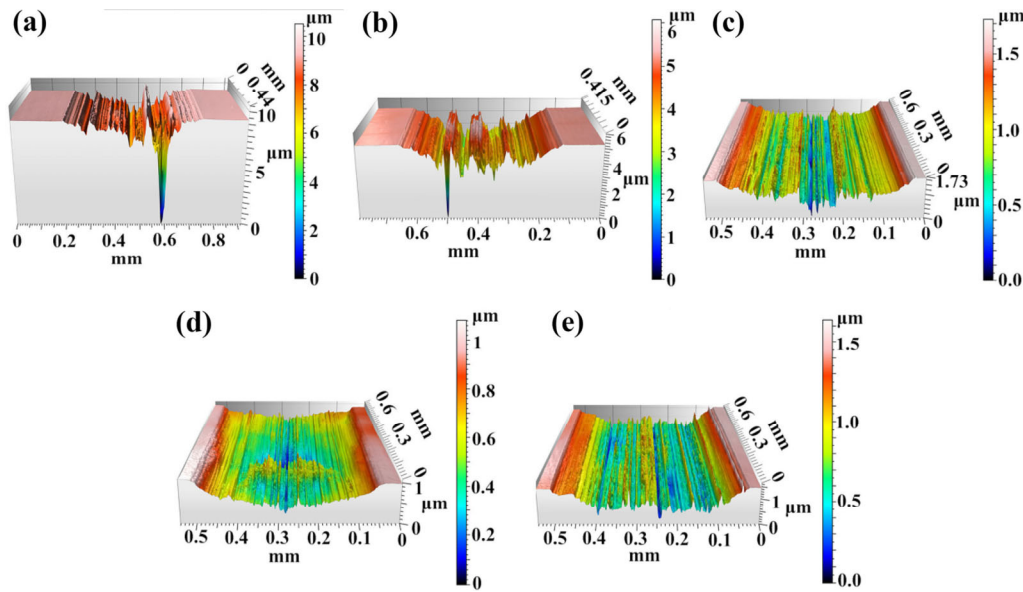


**Fig. 9** 3D cross profiles of worn surfaces lubricated by (a) PE-OA, and PE-OA with (b) 2%, (c) 3%, (d) 4%, and (e) 5% NOG.

which is the primary reason for the maximum depth observed in Fig. 8(d). In addition, the slight increase in WV and COF when the NOG content increases to 5% shows that the optimum concentration of NOG in PE-OA in terms of tribological performance is 4%. The low values of COF and WV, together with the smooth lubrication process, indicate the excellent lubrication performance of PE-OA gel lubricant, which might be attributed to the formation of boundary lubricating film.

### 3.6.3 Tribological performance of PEG400 gel lubricants

As shown in Fig. 10, NOG is also effective in improving the tribological performance of FEG400 oils, with an optimal concentration of about 4%. In addition, the NOG was found to be more efficient for wear reduction

in PEG oils because the WV was remarkably decreased (by more than 87%) compared with that of blank oil at the optimum adding concentration, as shown in Fig. 10.

## 3.7 Surface morphology analysis

### 3.7.1 Surface morphology analysis of LP gel lubricants

Figure 11 shows that when LP base oil and LP gel with 1 wt%, 3 wt%, and 4 wt% NOG content were used for lubrication, the worn surface showed the largest damage area with deep furrows and numerous micro-pits, a typical appearance caused by abrasive wear and adhesive wear. Figure 11(c) shows the smooth and regular shallow grooves on the worn scar when lubricated using LP-2% NOG gel. This means the direct

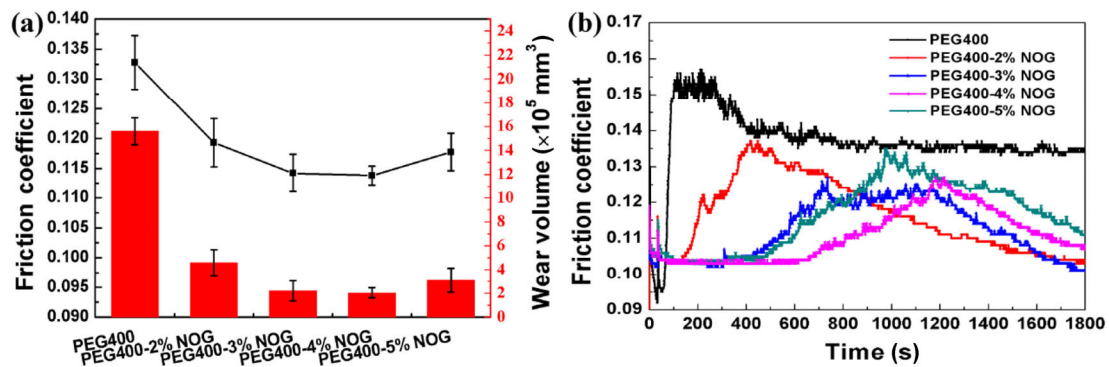


**Fig. 10** (a) Average COF and WV, (b) evolution of COF/time lubricated by the PEG400 and corresponding gel lubricants at room temperature (SRV: load = 100 N, stroke = 1 mm, frequency = 25 Hz, and duration = 30 min).

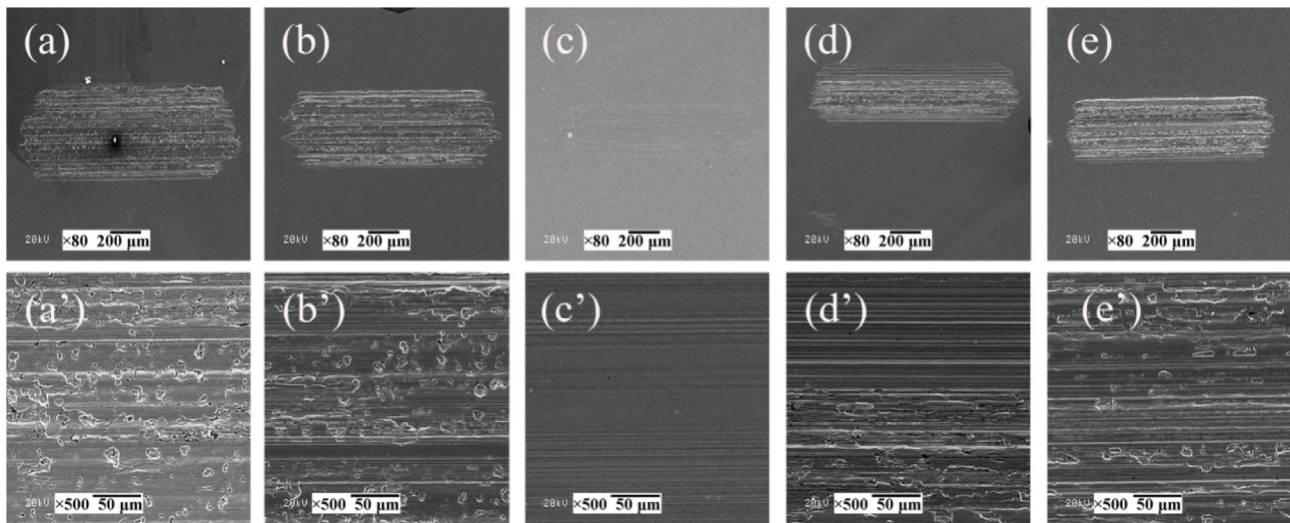


**Fig. 11** SEM images of worn surfaces lubricated by (a, a') LP, (b, b') LP-1% NOG, (c, c') LP-2% NOG, (d, d') LP-3% NOG, and (e, e') LP-4% NOG (magnification in the top panels is 80 $\times$ , and on the bottom panels is 500 $\times$ ; load = 50 N, stroke = 1 mm, frequency = 25 Hz, and duration = 30 min).

contact of friction pair is effectively avoided by 2 wt% NOG, along with the alleviation of micro-pits, indicating the formation of continuous and effective boundary lubricating film with 2 wt% NOG.

### 3.7.2 Surface morphology analysis of PE-OA gel lubricants

Figure 12 shows the SEM micrographs and 3D profile of worn scars lubricated by PE-OA-based lubricants. The surface morphologies of blank PE-OA (in Fig. 12(a)

and 12(a')) show severe damage with a wide furrow and large area of delamination. The obvious surface damage disappears completely when the NOG content reaches 3% (Figs. 12(c) and 12(c')), just showing shallow narrow grooves and some honeycombed abrasion. The worn surface is slightest and smoothest when lubricated by PE-OA-4% NOG (Figs. 12(d) and 12(d')), which is in agreement with the finding in Fig. 8. Furthermore, the size and the depth of the worn

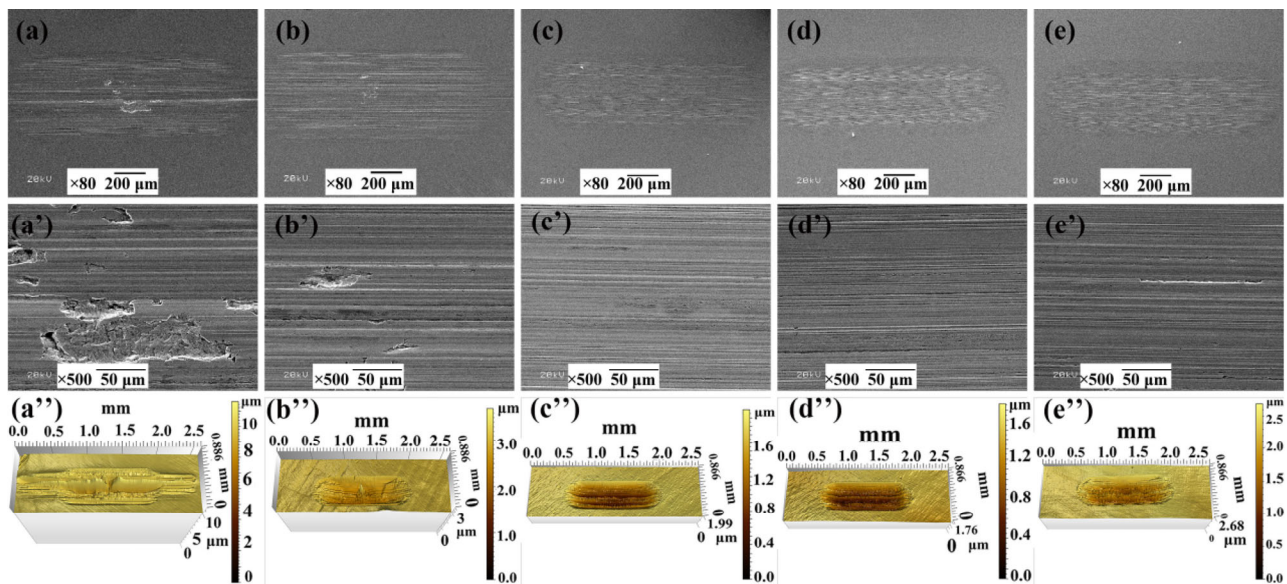


**Fig. 12** SEM and 3D optical microscopic morphologies of worn surfaces lubricated by (a, a', a'') PE-OA, (b, b', b'') PE-OA-2% NOG, (c, c', c'') PE-OA-3% NOG, (d, d', d'') PE-OA-4% NOG, and (e, e', e'') PE-OA-5% NOG (magnification in the top panels is 80 $\times$ , and in the middle panels is 500 $\times$ ; load = 300 N, stroke = 1 mm, frequency = 15 Hz, and duration = 30 min).



scar shown in corresponding 3D optical microscopic images (Figs. 12(a'')–12(e'')) are dramatically decreased when lubricated by PE-OA-4% NOG compared with that by PE-OA. Together with previous data of COF and WV, 4% NOG is the most optimum concentration for PE-OA to reduce the friction and alleviate wear.

### 3.7.3 Surface morphology analysis of PEG400 gel lubricants

Figures 13(a) and 13(a') show that the worn scar lubricated by pure PEG400 exhibits severe scuffing with wide and deep grooves. Upon lubrication by PEG400-4% NOG gel, the worn surface exhibits the least damage, with a regular and smoothest morphology. The anti-wear performances are further corroborated by 3D microscopic images (Figs. 13(a'')–13(e'')). The width and depth of worn scar lubricated by PEG400-4% NOG are smaller than that of other PEG400-based lubricants. Combined with the data for COF and WV, 4% is the optimal concentration of NOG for PEG400 oil in terms of wear and friction reduction.

## 3.8 Surface composition analysis of gel lubricants

### 3.8.1 Surface composition analysis of PE-OA gel lubricants

XPS, an effective tool to explore the composition and

chemical state of an element, was used to analyze the chemical change in worn scars after the friction-generating process. Figure 14 shows the XPS spectra of NOG gelator and worn scars lubricated by PE-OA-based gel lubricants. The O1s peaks at 531.15 eV, 532.11 eV, and 532.8 eV were respectively ascribed to the  $-C=O$ ,  $-OH$ , and  $-C-O-$  groups in the NOG molecule [23, 24]. Integrated with the peaks of Fe2p at approximately 723 eV and 710 eV, the O1s peaks of worn scar lubricated by neat PE-OA at about 531 eV and 529 eV were deduced to be oxide products of iron [25, 26]. The apparent new peak of O1s on the worn scar lubricated by PE-OA-4% NOG (532 eV) could be ascribed to the  $-OH$  group [23]. Combined with the Fe2p and O1s spectra of worn scar lubricated by PE-OA-4% NOG, a robust and compact iron oxide film, likely consisting of  $Fe_2O_3$ ,  $Fe(OH)O$ ,  $FeOOH$ ,  $FeO$ , and  $Fe_3O_4$ , was formed during the lubrication process [27–29]. In addition, the N1s peaks of NOG shifted to 399.6 and 400.5 eV after friction, which was ascribed to the formation of  $-C-N-$  group and nitrogen oxides or nitrates [30, 31]. Based on the above analysis, it could be concluded that the tribo-film containing organic oxides, iron oxides, and nitrogen oxides or nitrates could form during the lubrication process, which is related to the improved tribological performances.

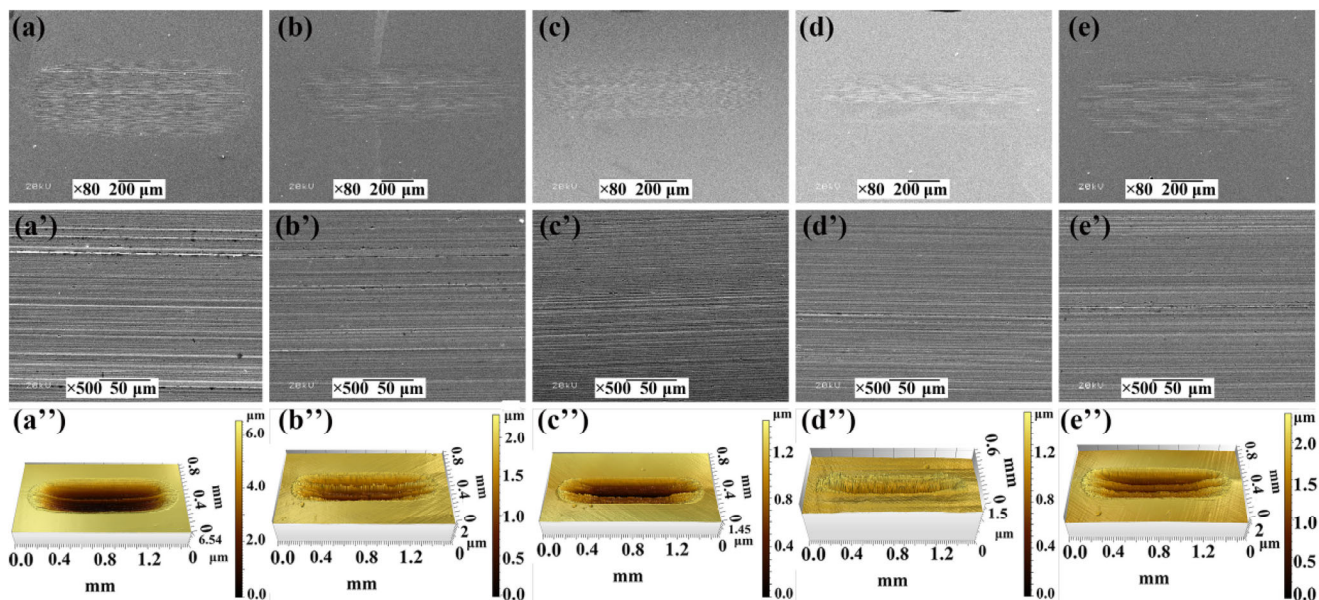


**Fig. 13** SEM and 3D optical microscopic morphologies of worn surfaces lubricated by (a, a', a'') PEG400, (b, b', b'') PEG400-2% NOG, (c, c', c'') PEG400-3% NOG, (d, d', d'') PEG400-4% NOG, and (e, e', e'') PEG400-5% NOG (magnification in the top panels is 80 $\times$ , and in the middle panels is 500 $\times$ ; load = 100 N, stroke = 1 mm, frequency = 25 Hz, and duration = 30 min).

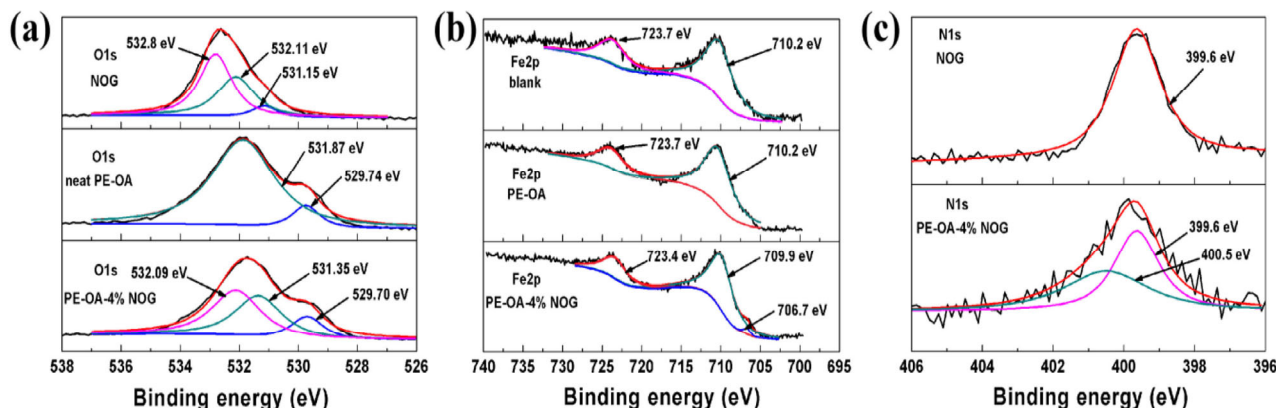


**Fig. 14** XPS spectra of (a) O1s of NOG and worn scars lubricated by neat PE-OA and PE-OA-4% NOG; (b) Fe2p of blank steel block and worn scars lubricated by neat PE-OA and PE-OA-4% NOG; (c) N1s of NOG and worn scars lubricated by PE-OA-4% NOG.

### 3.8.2 Surface composition analysis of LP gel lubricants

From the XPS spectra of LP-based gels presented in Fig. 15, it could be concluded that the NOG gelator has a similar lubricating mechanism as it does in PE-OA oil. The robust tribochemical films composed of organic oxides, iron oxides and nitrogen oxides or nitrates are generated on the sliding interfaces during friction, which is conducive to the tribological performance.

### 3.8.3 Surface composition analysis of PEG400 gel lubricants

The peaks of O1s spectrum of the worn scars lubricated by PEG400 and PEG400-4% NOG (Fig. 16) were similar to each other (all about 529.7 eV, 531 eV, and 532 eV), which might be attributed to the similar structures of PEG400 and NOG molecules. The polar hydroxyl groups present in NOG served to enhance the

lubricating effect of PEG400 by forming the same friction-reduced products. The difference of N1s peak between NOG and the worn scars lubricated by PEG400-4% NOG directly demonstrates the tribochemical reactions that take place upon lubrication by PEG400-4% NOG, which might be ascribed to the formation of nitrogen oxides or nitrates.

### 3.9 The lubricating mechanism of gel lubricants

The three types of gel lubricants showed a similar variation in the lubrication performance with a change in NOG concentration, with all exhibiting a decrease first and then an increase in COF and WV. However, the LP-based gel lubricants show the most apparent fluctuation of COF/WV values with the increase in NOG content compared with those of PEG400 and PE-OA gel lubricants, which is attributed to the

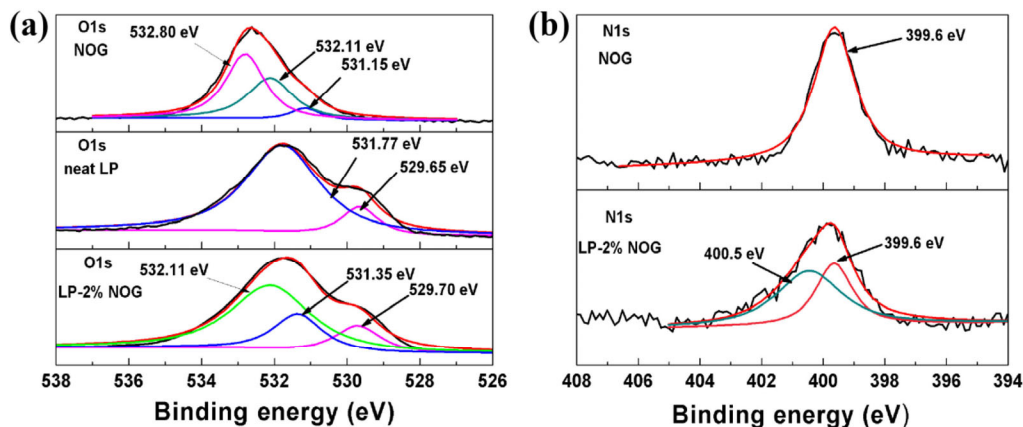


**Fig. 15** XPS spectra of (a) O1s of NOG and worn scars lubricated by neat LP and LP-2% NOG; (b) N1s of NOG and worn scar lubricated by LP-2% NOG.

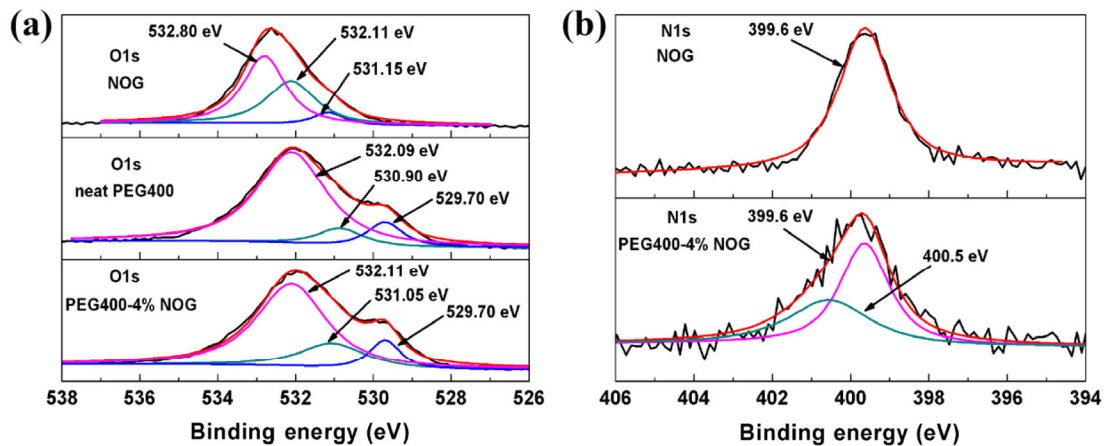


**Fig. 16** XPS spectra of (a) O1s of NOG and worn scars lubricated by neat PEG400 and PEG400-4% NOG; (b) N1s of NOG and worn scar lubricated by PEG400-4% NOG.

different properties of three types of base oil. In order to clarify the lubricating mechanism, it is necessary to identify the lubrication state of the system first. We take the LP as an example to demonstrate that the lubrication regime of friction contacts under the test condition belongs to the boundary lubricating state, as shown in the ESM. This means that the variation in viscosity due to the change in NOG content of the gel lubricant could not affect the lubrication performance strongly, and that physical adsorption and chemical reaction of the NOG gelator during the lubricating process are the main factors that determine the lubrication performance under the test condition [32].

In the initial stage before sliding starts, the gel lubricant cannot flow due to the immobilization by NOG gelator. As the sliding starts and continues, the base oil and NOG gelator could flow due to the shear-thinning property of the gel lubricant. At this stage, the released NOG molecules interact with the friction interface to exert the lubricating effect, and a higher content of NOG is beneficial for building the continuous boundary lubricating film. However, at the same time, the storage moduli ( $G'$ ) and the corresponding critical stress increase with the content of NOG, indicating that the mechanical stability and resistance to flow of LP gels could be effectively enhanced with increasing NOG concentration. Therefore, for tribological application, there should be an optimal NOG concentration to balance the boundary lubrication

ability and flow ability of gel lubricants.

Based on above discussion, the transformation from gel to sol under shear is important for the studied gel lubricants. Taking the example of LP gel lubricants, according to their lubrication performance shown in Figs. 7(a) and 7(b), the values of mean COF and wear volume gradually decrease to the lowest when the NOG content reaches to 2 wt%, which might be related with the formation of continuous and effective boundary lubricating film of NOG gelator at this concentration, as shown in Fig. 17II. However, when the NOG content increases further, the lubrication performance becomes worse, which might be due to the increased mechanical strength and decreased flow ability of the LP gel lubricants, as indicated by the increased  $G'$  and critical stress during the rheological analysis in Fig. S1 in the ESM. In such a situation, the gel (base oil and NOG gelator) is prone to be squeezed out of the contact area rather than spreading on the friction surface during the initial sliding stage (Fig. 17III), resulting in a starved lubricating state with a defective boundary film. The speculation could also be confirmed by the COF curve of the gel lubricants with 3 wt% and 4 wt% NOG. Thus, the LP with optimal NOG content would lead to the “optimal rheological property” and the “proper mechanical strength” of the gel lubricant, which finally balance the need for constructing the effective NOG boundary film and the need for the flow ability of gel system under shear, thus, finally providing the optimal lubrication performance.

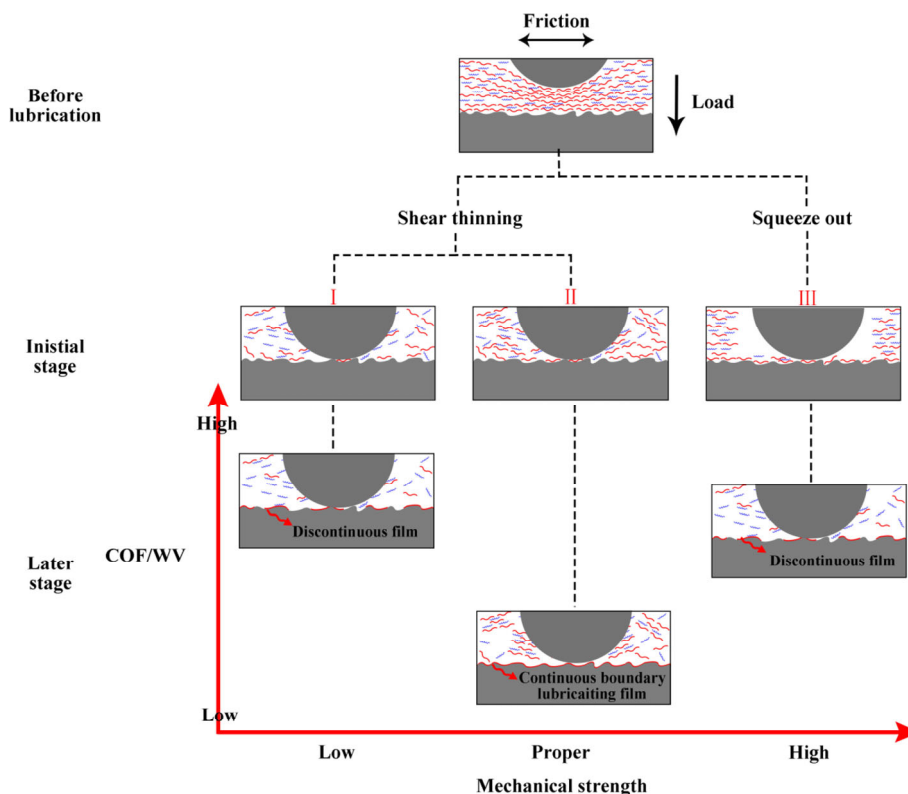


**Fig. 17** Schematic diagram of the lubricating mechanism of the prepared gel lubricants.

## 4 Conclusions

In this study, three types of gel lubricants with improved lubrication performance were prepared by gelling the PE-OA, PEG400, and LP base oils with NOG gelator. As confirmed by the IR spectra, the gelation is driven by the hydrogen bonds between the hydroxyl groups and carbonyl groups in NOG molecules. Moreover, the addition of NOG could improve the thermal stability of the base oils, as demonstrated by the TGA analysis. The rheological data indicated that the prepared PEG400, LP, and PE-OA gels possess good mechanical strength, good tolerance ability, and shear-thinning properties. Tribological evaluation shows that NOG, as an additive in base oils, could remarkably reduce the friction and wear. A plausible mechanism was proposed for the improvement in lubrication performance, related to the proper mechanical strength of the gel and the formation of a lubricating boundary film on the worn surface. These results indicate that NOG is a potential gelator for preparing gel lubricants with excellent tribological properties and environment-friendly characteristics.

## Acknowledgements

The authors are grateful for the financial support from the National Key R&D Program of China (No. 2018YFB0703802), National Natural Science Foundation of China (Nos. 51405477, 21972153, and 51675512), Youth Innovation Promotion Association of CAS (No. 2018454), and the Gansu province science and technology plan (No. 18ZD2WA011).

**Electronic Supplementary Material:** Supplementary Material is available in the online version of this article at <https://doi.org/10.1007/s40544-019-0316-0>.

**Open Access:** This article is licensed under a Creative Commons Attribution 4.0 International License, which permits use, sharing, adaptation, distribution and reproduction in any medium or format, as long as you give appropriate credit to the original author(s) and the source, provide a link to the Creative Commons licence, and indicate if changes were made.

The images or other third party material in this article are included in the article's Creative Commons

licence, unless indicated otherwise in a credit line to the material. If material is not included in the article's Creative Commons licence and your intended use is not permitted by statutory regulation or exceeds the permitted use, you will need to obtain permission directly from the copyright holder.

To view a copy of this licence, visit <http://creativecommons.org/licenses/by/4.0/>.

## References

- [1] Holmberg K, Andersson P, Erdemir A. Global energy consumption due to friction in passenger cars. *Tribol Int* **47**: 221–234 (2012)
- [2] Zhou F, Liang Y, Liu W. Ionic liquid lubricants: Designed chemistry for engineering applications. *Chem Soc Rev* **38**(9): 2590–2599 (2009)
- [3] Klein J. Hydration lubrication. *Friction* **1**(1): 1–23 (2013)
- [4] Canbulut F, Sinanoğlu C, Yildirim Ş. Neural network analysis of leakage oil quantity in the design of partially hydrostatic slipper bearings. *Ind Lubr Tribol* **56**(4): 231–243 (2004)
- [5] Fan X, Xia Y, Wang L. Tribological properties of conductive lubricating greases. *Friction* **2**(4): 343–353 (2014)
- [6] Lugt P M. A review on grease lubrication in rolling bearings. *Tribol T* **52**(4): 470–480 (2009)
- [7] Cai M, Liang Y, Zhou F, Liu W. Functional ionic gels formed by supramolecular assembly of a novel low molecular weight anticorrosive/antioxidative gelator. *J Mater Chem* **21**(35): 13399–13405 (2011)
- [8] Cai M, Liang Y, Zhou F, Liu W. Tribological properties of novel imidazolium ionic liquids bearing benzotriazole group as the antiwear/anticorrosion additive in poly (ethylene glycol) and polyurea grease for steel/steel contacts. *ACS Appl Mater Inter* **3**(12): 4580–4592 (2011)
- [9] Gabriele A, Spyropoulos F, Norton I. A conceptual model for fluid gel lubrication. *Soft Matter* **6**(17): 4205–4213 (2010)
- [10] Zhang Z, Liu J, Wu T, Xie Y. Effect of carbon nanotubes on friction and wear of a piston ring and cylinder liner system under dry and lubricated conditions. *Friction* **5**(2): 147–154 (2017)
- [11] Takahashi K, Shitara Y, Kaimai T, Kanno A, Mori S. Lubricating properties of TR gel-lube—Influence of chemical structure and content of gel agent. *Tribol Int* **43**(9): 1577–1583 (2010)
- [12] Yu Q, Huang G, Cai M, Zhou F, Liu W. *In situ* zwitterionic supramolecular gel lubricants for significantly improved tribological properties. *Tribol Int* **95**: 55–65 (2016)
- [13] Yu Q, Li D, Cai M, Zhou F, Liu W. Supramolecular gel lubricants based on amino acid derivative gelators. *Tribol Lett* **61**(2): 16 (2016)
- [14] Huang G, Yu Q, Cai M, Zhou F, Liu W. Highlighting the effect of interfacial interaction on tribological properties of supramolecular gel lubricants. *Adv Mater Interfaces* **3**(3): 1500489 (2016)
- [15] Li K, Wang X, Shan L, Jin Q, Niu X, Liu Y. Synthesis of pentaerythritol oleate. *China Oils and Fats* **12**: 016 (2007)
- [16] Mehlretter C, Furry M, Mellies R, Rankin J. Surfactants and detergents from sulfated N-alkyl-gluconamides. *J Am Oil Chem Soc* **29**(5): 202–207 (1952)
- [17] Yoza K, Amanokura N, Ono Y, Akao T, Shinmori H, Takeuchi M, Shinkai S and Reinhoudt D. Sugar-integrated gelators of organic solvents—their remarkable diversity in gelation ability and aggregate structure. *Chem Weinheim Eur J* **5**: 2722–2729 (1999)
- [18] Hanabusa K, Fukui H, Suzuki M, Shirai H. Specialist gelator for ionic liquids. *Langmuir* **21**(23): 10383–10390 (2005)
- [19] Graener H, Ye T, Laubereau A. Ultrafast dynamics of hydrogen bonds directly observed by time-resolved infrared spectroscopy. *J Chem Phys* **90**(7): 3413–3416 (1989)
- [20] Teo L, Chen C, Kuo J. Fourier transform infrared spectroscopy study on effects of temperature on hydrogen bonding in amine-containing polyurethanes and poly(urethane–urea)s. *Macromolecules* **30**(6): 1793–1799 (1997)
- [21] Ilanko A K, Vijayaraghavan S. Wear behavior of asbestos-free eco-friendly composites for automobile brake materials. *Friction* **4**(2): 144–152 (2016)
- [22] Cartigueyen S, Mahadevan K. Wear characteristics of copper-based surface-level microcomposites and nanocomposites prepared by friction stir processing. *Friction* **4**(1): 39–49 (2016)
- [23] Espinosa T, Jiménez M, Sanes J, Jiménez A, Iglesias M and Bermudez M. Ultra-low friction with a protic ionic liquid boundary film at the water-lubricated sapphire–stainless steel interface. *Tribol Lett* **53**(1): 1–9 (2014)
- [24] Martin J, Matta C, Bouchet M, Forest C, Mogne T, Dubois T and Mazarin M. Mechanism of friction reduction of unsaturated fatty acids as additives in diesel fuels. *Friction* **1**(3): 252–258 (2013)
- [25] Han Y, Qiao D, Guo Y, Feng D, Shi L. Influence of competitive adsorption on lubricating property of phosphonate ionic liquid additives in PEG. *Tribol Lett* **64**(2): 22 (2016)
- [26] Yang G, Zhao J, Cui L, Song S, Zhang S, Yu L, Zhang P. Tribological characteristic and mechanism analysis of borate ester as a lubricant additive in different base oils. *RSC Adv* **7**(13): 7944–7953 (2017)
- [27] Xia Y, Xu X, Feng X, Chen G. Leaf-surface wax of desert plants as a potential lubricant additive. *Friction* **3**(3): 208–213 (2015)

- [28] Song Z, Liang Y, Fan M, Zhou F, Liu W. Lithium-based ionic liquids as novel lubricant additives for multiply alkylated cyclopentanes (MACs). *Friction* **1**(3): 222–231 (2013)
- [29] NIST X-ray photoelectron spectroscopy (XPS) database. <http://srdata.nist.gov/xps/>.
- [30] Lu Q, Wang H, Ye C, Liu W, Xue Q. Room temperature ionic liquid 1-ethyl-3-hexylimidazolium-bis (trifluoromethylsulfonyl)-imide as lubricant for steel–steel contact. *Tribol Int* **37**(7): 547–552 (2004).
- [31] Otero I, López E R, Reichelt M; Fernández J. Tribo- chemical reactions of anion in pyrrolidinium salts for steel–steel contact. *Tribol Int* **77**: 160–170 (2014)



**Ruochong ZHANG.** She is studying for her Ph.D. degree in materials science in Lanzhou Institute of

Chemical Physics, China. Her research interests include lubricating additives and gel lubricants.



**Lei SHI.** She received her Ph.D. degree in physical chemistry from Lanzhou Institute of Chemical Physics, China, in 2005. After then, she joined the State Key Laboratory

of Solid Lubrication at Lanzhou Institute of Chemical Physics. Her current position is an associate professor. Her research is focused on the novel nano-structured materials with excellent mechanical, tribological behaviors.



**Meirong CAI.** She got her Ph.D. degree in 2012 at the Lanzhou Institute of Chemical Physics. She is an associate professor at the State Key Lab of Solid Lubrication in

Lanzhou Institute of Chemical Physics, CAS. She has authored or co-authored more than 60 journal papers. Her research interests are ionic liquids lubricants and supramolecular gel lubricants.